Materials Today Bio 38 (2026) 103199

Contents lists available at ScienceDirect

Materials Today Bio

journal homepage: www.journals.elsevier.com/materials-today-bio

Auto-loaded polydopamine-M2 exosomes as an antioxidative nanoscavenger for lupus erythematosus therapy

Huiyuan Ye [a], Shufan Hou [a], Xingyu Li [b], Yujuan Zhu [a,*], Zhifeng Gu [a,**], Mei Yang [a,***]

[a] Department of Rheumatology, Research Center of Clinical Medicine, Research Center of Immunology, Affiliated Hospital of Nantong University, Medical School of Nantong University, Nantong, 226001, China
[b] Medical School of Nantong University, Nantong, 226001, China

ARTICLE INFO

Keywords:
M2 exosome
Auto-loaded polydopamine
Antioxidative nanoscavenger
Systemic immunotherapy
Lupus erythematosus

ABSTRACT

Systemic lupus erythematosus (SLE) is a chronic autoimmune disease characterized by multisystem inflammation and immune dysregulation, predominantly affecting women of reproductive age. Current treatments, including antimalarials, corticosteroids, and immunosuppressants, often entail long-term toxicity. To address this, we developed an auto-loaded polydopamine-M2 exosome system (M2/pEXO) as an antioxidative nanoscavenger for SLE therapy. Ultrasmall PDA nanoparticles facilitated M2 macrophage polarization and were autonomously encapsulated into exosomes during polarization, yielding M2/pEXO with enriched protein content and enhanced cellular uptake. Proteomic analysis indicated that M2/pEXO cargo proteins are involved in cellular energy metabolism and inflammatory regulation, underpinning its immunomodulatory and antioxidant functions. Compared with conventional M2 EXO, M2/pEXO exhibited superior antioxidative and anti-inflammatory effects, reducing M1 macrophage polarization and pro-inflammatory cytokine secretion while promoting regulatory T cell expansion. In a murine SLE model, M2/pEXO significantly alleviated lupus nephritis, attenuating renal immune infiltration, glomerular mesangial proliferation, proteinuria, serum creatinine, and anti-dsDNA autoantibody levels, without detectable toxicity. The platform elevates M2 EXO from mere anti-inflammatory carriers to an integrated nanoscavenger system capable of targeted delivery, oxidative stress scavenging, and immunomodulation. This auto-loaded, naturally engineered strategy presents a safe and effective therapeutic approach for SLE and potentially other chronic inflammatory diseases.

1. Introduction

Systemic lupus erythematosus (SLE) is a chronic, relapsing autoimmune disorder that afflicts multiple organs and predominately affects women of child-bearing age. Its pathogenesis is multifactorial—genetic, immune, hormonal and environmental cues converge to drive autoreactivity [1,2]. Reactive oxygen species (ROS) maintain a dynamic equilibrium with intracellular antioxidant systems and participate in critical signaling pathways. However, excessive ROS production coupled with impaired clearance capacity, including superoxide anion, hydrogen peroxide, and hydroxyl radicals, significantly increases the risk of SLE onset and exacerbates disease severity. Existing research indicates that ROS are associated with the initiation and progression of inflammatory responses, serving as key upstream drivers in SLE pathogenesis [3,4]. Current therapies (corticosteroids, antimalarials, immunosuppressants and biologics such as belimumab and anifrolumab) can achieve remission, curb morbidity and enhance quality of life [5,6], yet organ toxicities, heterogeneous disease biology and limited evidence for some agents remain major hurdles [7]. Although conventional therapies can partially control the disease, their long-term use entails significant toxicity and limited efficacy in refractory or severe cases, making systemic immunotherapy an essential direction to meet clinical needs [8,9]. Nano-material drug delivery technology has been applied in therapeutic research for various diseases, but treatment strategies targeting the characteristic high levels of ROS in SLE remain understudied.

Therefore, we propose a ROS nanoscale scavenger based on the antioxidant properties of nanomaterials for the treatment of SLE.

* Corresponding author.
** Corresponding author.
*** Corresponding author.
E-mail addresses: yujuanzhu@ntu.edu.cn (Y. Zhu), guzf@ntu.edu.cn (Z. Gu), yangmei@ntu.edu.cn (M. Yang).

https://doi.org/10.1016/j.mtbio.2026.103199
Received 19 December 2025; Received in revised form 22 April 2026; Accepted 2 May 2026
Available online 2 May 2026

Exosomes, as a promising natural nanomaterial, are cell-derived nanovesicles (30–200 nm) that are actively released into the extracellular space. They can deliver bioactive molecules such as miRNAs, lipids, and proteins to facilitate intercellular communication and regulate the functions of recipient cells [10,11]. They act as mediators of intercellular communication, impacting both healthy and diseased states [12]. As naturally occurring vesicles, exosomes have the characteristics of low immunogenicity, nanoscale structure, multi-target synergistic action, thereby being widely applied in the fields of inflammation regulation, tissue repair and regeneration [13,14]. However, exosomes face significant limitations due to their functional singularity-they primarily serve as intercellular "messengers" rather than multi-functional "repair agents", restricting their therapeutic scope to signaling modulation rather than direct tissue regeneration or complex disease intervention [15,16]. Currently, a vast array of novel materials has been developed, exhibiting diverse morphologies and encompassing both natural and synthetic types [17,18]. With their unique size effects, high specific surface area, excellent biocompatibility, multifunctionality, and ease of modification, these materials hold great promise in biomedicine, materials science, and energy applications [19,20]. For example, the small-scale properties of nanomaterials can be precisely controlled for applications in biomedical fields such as targeted drug delivery and disease diagnostic imaging [21,22]. Additionally, nanomaterials exhibit multiple biological activities including anti-inflammatory and antioxidant effects [23,24]. However, these nanomaterials are often foreign substances that can easily trigger immune responses within the body, potentially leading to damage to the organism [25,26]. Therefore, by incorporating nanomaterials to construct exosome complexes, a promising therapeutic strategy may be offered through natural mechanisms, particularly for immune disorders such as systemic lupus erythematosus (SLE).

In this study, we present an auto-loaded polydopamine-M2 exosome system (M2/pEXO) as an antioxidative nanoscavenger for targeted immunotherapy of systemic lupus erythematosus (SLE). Ultrasmall polydopamine (PDA) nanoparticles not only promote M2 macrophage polarization but also exert substantial immunomodulatory and cytokine-signaling functions. Following endocytosis by M2-polarized macrophages, these PDA nanoparticles are autonomously incorporated into exosomes during polarization, yielding M2/pEXO with enhanced protein content and improved cellular uptake capacity. Proteomic analysis revealed that cargo proteins in M2/pEXO are predominantly associated with cellular energy metabolism and inflammatory regulation—including oxidative stress response, mitochondrial oxidative phosphorylation, and immune-related pathways—thereby substantiating its integrated immunomodulatory and antioxidant properties. Compared with conventional M2 exosomes (M2 EXO), M2/pEXO demonstrated superior antioxidant and anti-inflammatory activity, as indicated by a reduced proportion of M1 macrophages and lower secretion of pro-inflammatory cytokines such as IL-6 and TNF-α, alongside promoted expansion of regulatory T cells (Tregs). In a murine SLE model, M2/pEXO effectively alleviated lupus nephritis pathology, attenuating renal immune cell infiltration and glomerular mesangial expansion. Moreover, treatment with M2/pEXO significantly reduced proteinuria, serum creatinine, anti-dsDNA autoantibody levels, and multiple pro-inflammatory cytokines. The system further modulated immune homeostasis by increasing Treg and M2 macrophage populations while reducing M1 macrophage prevalence. Collectively, this work establishes an engineered, naturally assembled exosome-based platform that leverages endogenous cellular mechanisms for targeted therapeutic delivery, offering a promising nanoscavenger strategy for SLE and related chronic inflammatory diseases.

2. Results and discussion

2.1. Preparation of PDA nanoparticles and characterization of M2/pEXO

Polydopamine (PDA) nanoparticles of extremely small size were prepared through the self-polymerization of dopamine and Michael addition reaction (see Fig. 1). Transmission electron microscopy (TEM) revealed that PDA consists of uniformly small spherical nanoparticles with an average diameter of 1.2 nm and a surface zeta potential of −3.74 mV, which are ideal for cellular uptake and subsequent packaging into exosomes (Fig. 2a–c). Owing to the intrinsic green fluorescence of PDA, we further characterized the synthesized nanoparticles by PL fluorescence spectroscopy. The spectrum revealed an excitation wavelength of ~450 nm (Fig. S1b), confirming the intrinsic fluorescence.

To naturally synthesize M2/pEXO, bone marrow-derived macrophages (BMDM) were exposed to PDA and then differentiated into M2 macrophages. Following endocytosis and exocytosis, exosomes were collected with naturally loaded PDA. Nanoparticle tracking analysis (NTA) showed that isolated M2/pEXO exhibited a mean diameter of 184.7 nm and a zeta potential of -3.97 ± 0.47 mV, a profile virtually identical to that of M2 EXO (Figs. S1a and Fig. 2c). Transmission electron microscopy further confirmed their uniform nano-spherical morphology and smooth surface (Fig. 2d). To verify sample authenticity, Western blotting was performed for the exosomal markers CD9, TSG101 and CD63, using RAW264.7 cell lysate as a control. Compared with the lysate, M2 EXO preparations displayed strong signals for CD9, TSG101 and CD63, whereas the endoplasmic-reticulum marker calreticulin was absent (Fig. 2e). Meanwhile, the negative organelle marker GM130 was also absent. Regarding the expression of M2 markers CD163 and Arg-1, M2/pEXO showed comparable levels to M2 cells (Fig. S1e). To assess the natural loading of PDA into M2/pEXO, EXO were labeled with DiL dye, and M2/pEXO (red) was partially overlapped with PDA (green). The superimposed image of M2/pEXO signal (DIL labeled fluorescence) and PDA signal is displayed to determine whether they are co-located at the same position (Fig. 2h and i). Semi-quantitative assessment of PDA nanoparticle loading in M2/pEXO was performed using colocalization coefficient analysis. The results showed that the Pearson' s coefficient of the M2/pEXO group was 0.88, indicating strong co-localization between PDA and exosomal fluorescence, with approximately 88% of pixel intensity correlation attributed to spatial overlap (Fig. S5h). This confirms the successful generation of PDA-loaded exosomes that retain the typical morphology of conventional exosomes.

To explore the differences between EVs from M2 and M2/PDA sources, microBCA and NTA were used to measure their concentrations. The results showed a correlation between total EV protein content and particle concentration, with M2/pEXO having higher protein content than M2 EXO (Fig. 2f). By size determination, both were within the acceptable particle size range (Fig. 2g). The cellular uptake of M2/pEXO was investigated by co-culturing RAW264.7 cells with them for durations of 1, 2, 4, and 6 h. M2 EXO was mainly localized to the membrane, while M2/pEXO was predominantly visible in the perinuclear region (Fig. 2k). Quantitative colocalization analysis revealed that the M2/pEXO group exhibited a significantly higher Pearson's correlation coefficient for the perinuclear region than the M2 EXO group, indicating stronger fluorescence intensity correlation with this subcellular compartment (Fig. 2j). These results suggest that M2/pEXO may be engulfed by inflammatory cells through enhanced endocytosis, thereby achieving an anti-inflammatory effect. In lupus nephritis, immune-complex deposition and inflammatory factors upregulate adhesion molecules on glomerular endothelial cells, leading to barrier disruption, leukocyte activation, and persistent microvascular injury. Therefore, investigating the endocytosis of endothelial cells is of paramount importance for SLE therapy. To evaluate the endocytosis efficiency, different cell types were utilized, including human macrophage THP-1 cells, human umbilical vein endothelial cells and mouse macrophage RAW264.7 cells. Using precise spectral compensation in flow cytometry

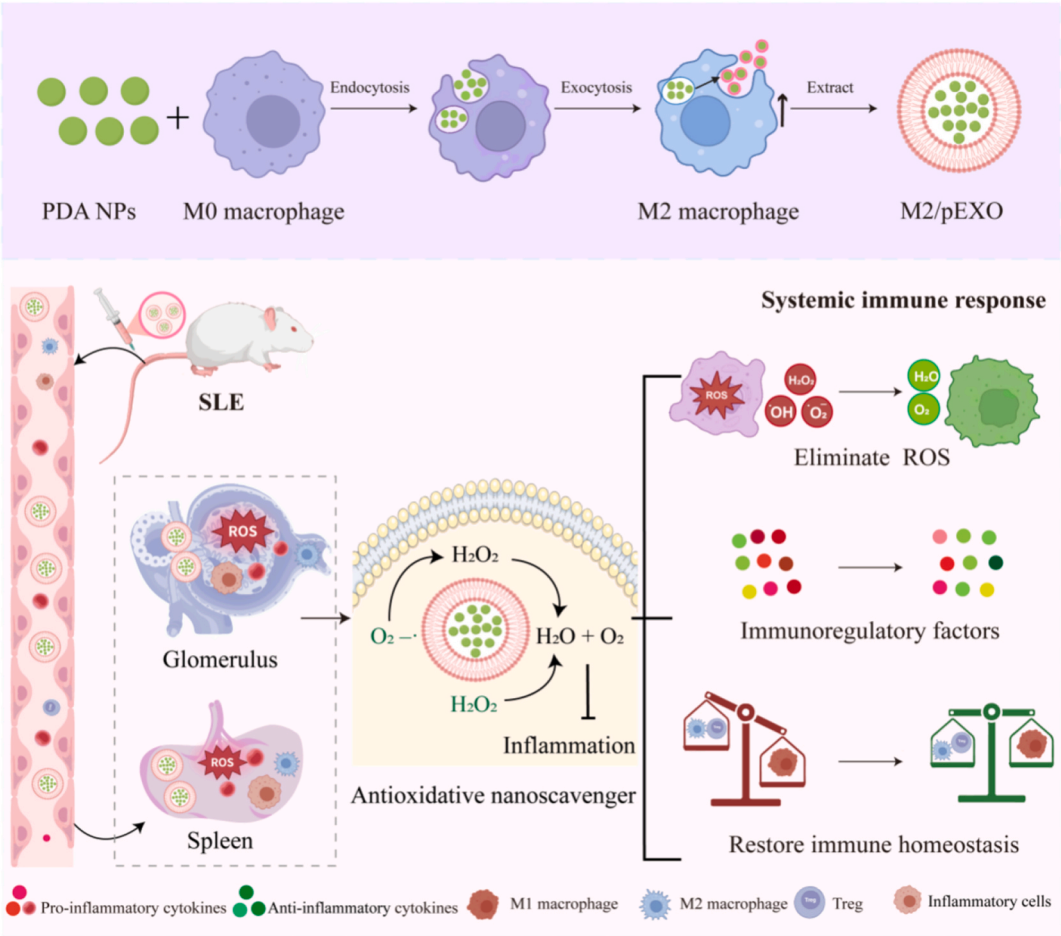

Fig. 1. Schematic diagram of auto-loaded polydopamine-M2 exosomes for SLE therapy. The novel dopamine-loaded M2 exosome system (M2/pEXO), synthesized via endocytosis–exocytosis cycling, exhibits superior antioxidant capacity and offers targeted immunotherapy for systemic lupus erythematosus (SLE).

experiments, we found that in HUVECs, the fluorescence intensity of M2/pEXO was higher than that of M2 EXO or free PDA (Fig. 2l–m, Fig. S5d-g), indicating that M2/pEXO possesses a markedly enhanced endocytic capacity.

2.2. Proteomic profiling of M2/pEXO

Given the differences in exosome contents and endocytosis, we next investigated the protein differences in exosomes via DIA proteomics sequencing. DIA proteomics identified 1627 proteins, with 236 showing significant changes in M2/pEXO (Fig. 3a). To explore the protein level differences between the two groups, DAVID 6.7 was used for KEGG pathway enrichment analysis. The results demonstrated that, relative to the control, the differentially expressed proteins identified in the M2/pEXO group were predominantly enriched in reactive oxygen species cGMP-PKG signaling pathway, thermogenesis, oxidative phosphorylation, AMPK signaling pathway, NOD-like receptor signaling pathway, ferroptosis, and neurodegenerative diseases-multiple diseases (Fig. 3b). Following cellular uptake of the PDA, it may influence cellular energy metabolism (such as by activating the AMPK pathway) and stress responses, thereby remodelling the secretory contents of exosomes to enrich them with proteins associated with antioxidant and immunomodulatory functions. GO analysis revealed that, relative to the control, the differentially expressed proteins identified in the M2/pEXO-treated samples showing significant enrichment for the ERBB signaling pathway, the epidermal growth factor receptor (EGFR) signaling pathway, protein tyrosine kinase activity, and active transmembrane transporter activity (Fig. S2a). Reactome analysis of differential proteins found immune-related and metabolism-related proteins to be highly enriched. In addition to immune and adaptive immune systems, activities like metabolic processes, Vamp2-associated secretory vesicle, plasma membrane transport, cytoplasmic recruitment of proteins to vesicles, small molecule transport, protein metabolism, cellular response to external stimuli, cytokine-related signaling in the immune system, and membrane-related transport were significantly enhanced, indicating possible alterations in M2/pEXO cell metabolism (Fig. 3d, Fig. S2b). These proteins are widely associated with energy metabolism amitochondrial function (HSD17B10, SLC25A13, HADHA, PHB2), inflammation and cell death (AK2, EPHX1, PLSCR3), organ damage related to nervous system diseases (ATP5F1C, NDUFB1, COX6C), and T/B cell differentiation and function (STAT3, VDAC1, PRKCD) (Fig. 3c and e). Protein (ABL1) involved in Ras/MAPK, PI3K/AKT and JAK/STAT signaling were also up-regulated. (Fig. 3e). In summary, the proteomic analysis suggests M2/pEXO with potential immunomodulatory effects.

2.3. Effect of PDA on M2 macrophage polarization

Based on the significant differences in exosomes, we next investigated the effects of PDA on M2 macrophage differentiation. FACS results showed that with the exposure of 50 μg/mL PDA, the proportion of M0 cells differentiating into M2 cells increased to 92.4%. When BMDMs were stimulated with various PDA concentrations, the $F4/80^{+}$ $CD206^{+}$ M2 cell proportion rose compared to the control group, indicating PDA delivery promotes M0 to M2 polarization (Fig. 4a). The M2 polarization effect of PDA exhibits concentration-dependent characteristics. M2 polarization demonstrates a saturation effect, with 50 μg/mL potentially

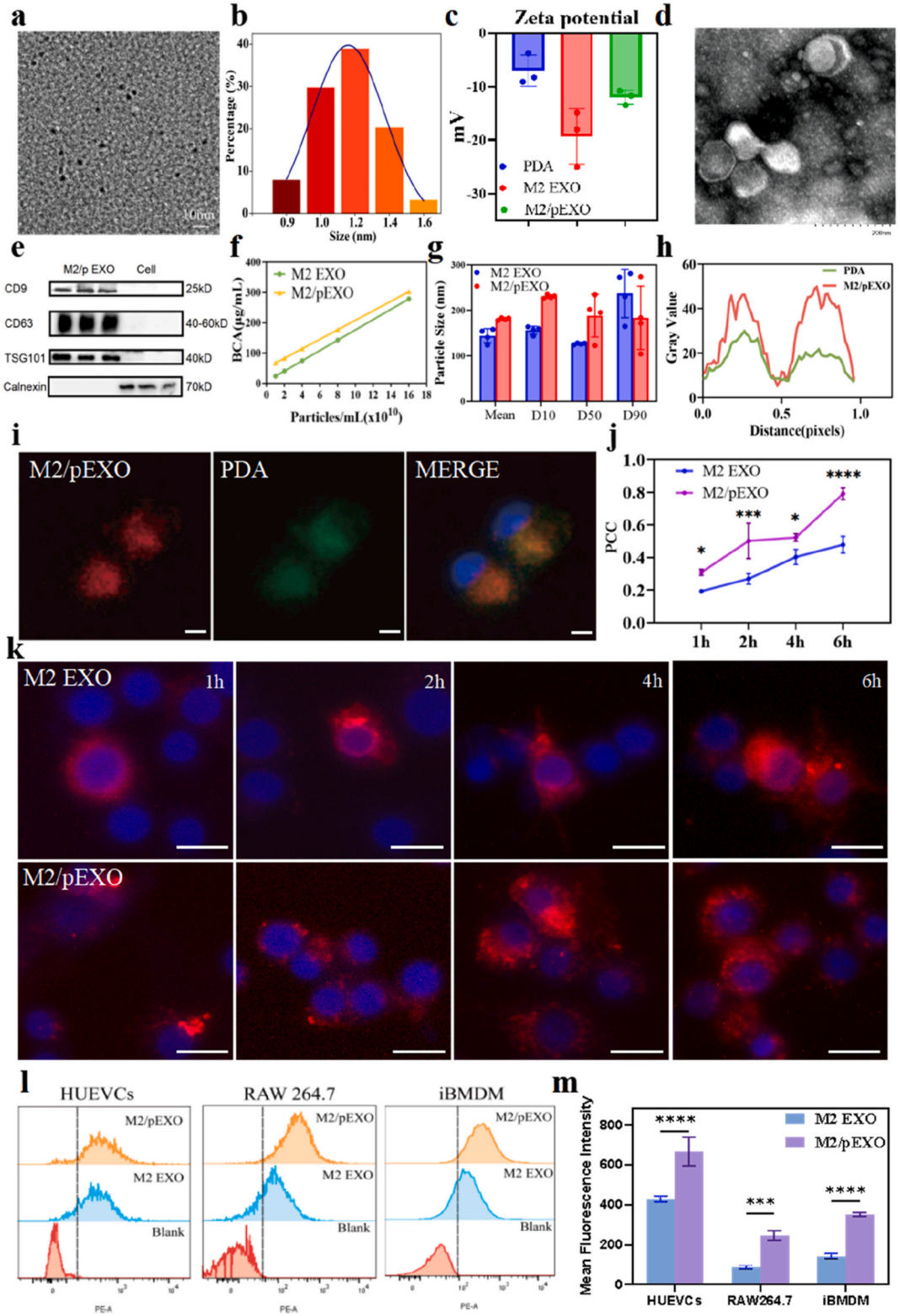

Fig. 2. **(a)** TEM images of PDA nanoparticles. (**b**) Size of PDA in PBS measured by DLS. (**c**) Zeta-potential of PDA, M2 EXO and M2/pEXO in PBS (n = 3). Data are presented as mean ± s.d. **(d)** TEM images of M2/pEXO. Scale bar, 200 nm. (**e**) WB of CD9, TSG101, CD63 and Calnexin. **(f)** Protein concentration measured by microBCA assay correlated with particle concentration measured by NTA (n = 5). **(g)** Size of M2 EXO and M2/pEXO in PBS measured by NTA. Percentiles (D10, D50, and D90) characterize the particle size distribution. **(h–i)** The statistical chart of the colocalization between PDA and M2/pEXO. Scale bars, 5 μm. (**j-k**) Representative microscopic images of RAW 264.7 cells engulfing M2/pEXO and M2 EXO, along with colocalization coefficient analysis. Scale bars, 10 μm. **(l)** The flow cytometry plots show the endocytosis of different exosomes by various cell types. **(m)** Assessed by flow cytometry, cellular uptake data are presented as Mean Fluorescence Intensity (MFI).

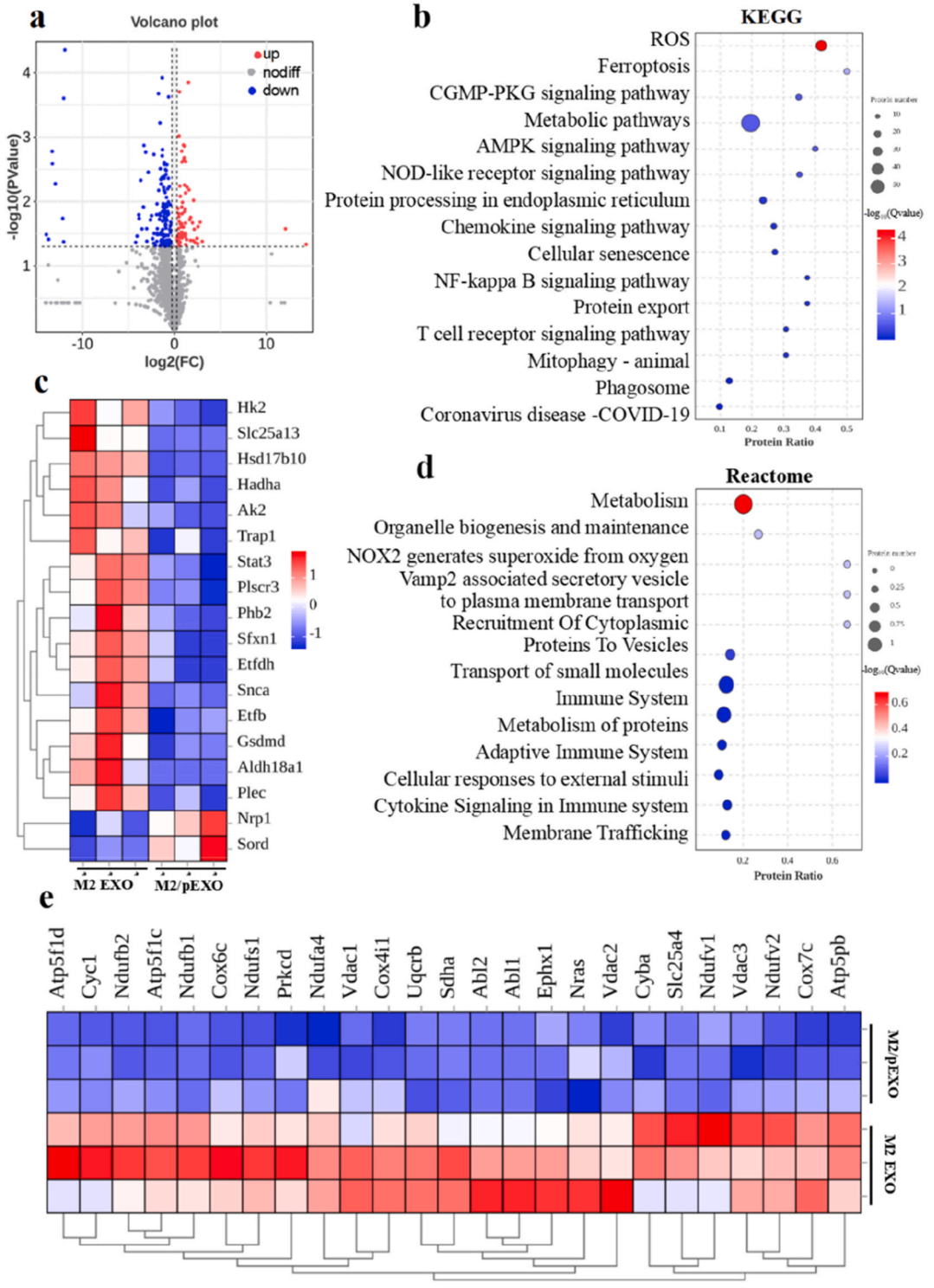

Fig. 3. (a) Volcano plot of proteomics sequencing of M2/pEXO and M2 EXO. **(b)** KEGG analysis of proteomics sequencing of M2/pEXO and M2 EXO. **(c, e)** Heatmap of differential protein expression related to immunity and metabolism in proteomics sequencing of M2/pEXO and M2 EXO. **(d)** Reactome pathway analysis of proteomics sequencing of M2/pEXO and M2 EXO.

achieving maximum induction efficiency; higher concentrations may not necessarily yield stronger effects, a phenomenon consistent with common biological observations. To delve deeper into the effects of PDA on BMDMs, we conducted transcriptomic sequencing on BMDMs with and without PDA stimulation. As shown in the volcano plot, compared to M2 group, M2/PDA group had 36 downregulated and 73 upregulated genes. GO analysis of DEGs showed that the M2/PDA group was enriched for ECM-related terms, cell proliferation and migration, oxidoreductase activity, vascular transport, regulation of vascular development, and modulation of angiogenesis (Fig. 4c, Fig. S3a). The top 10 GO terms, ranked by *p* value, highlighted significant enrichment in responses to external stimuli, ECM, and immune regulation (Fig. 4b). KEGG analysis showed that upregulated DEGs after PDA stimulation were enriched in pathways, such as PPAR signaling, TGF-β signaling, and the PI3K-Akt pathway. Reactome analysis also found upregulated genes enriched in ECM organization, PDGF-related processes, viral

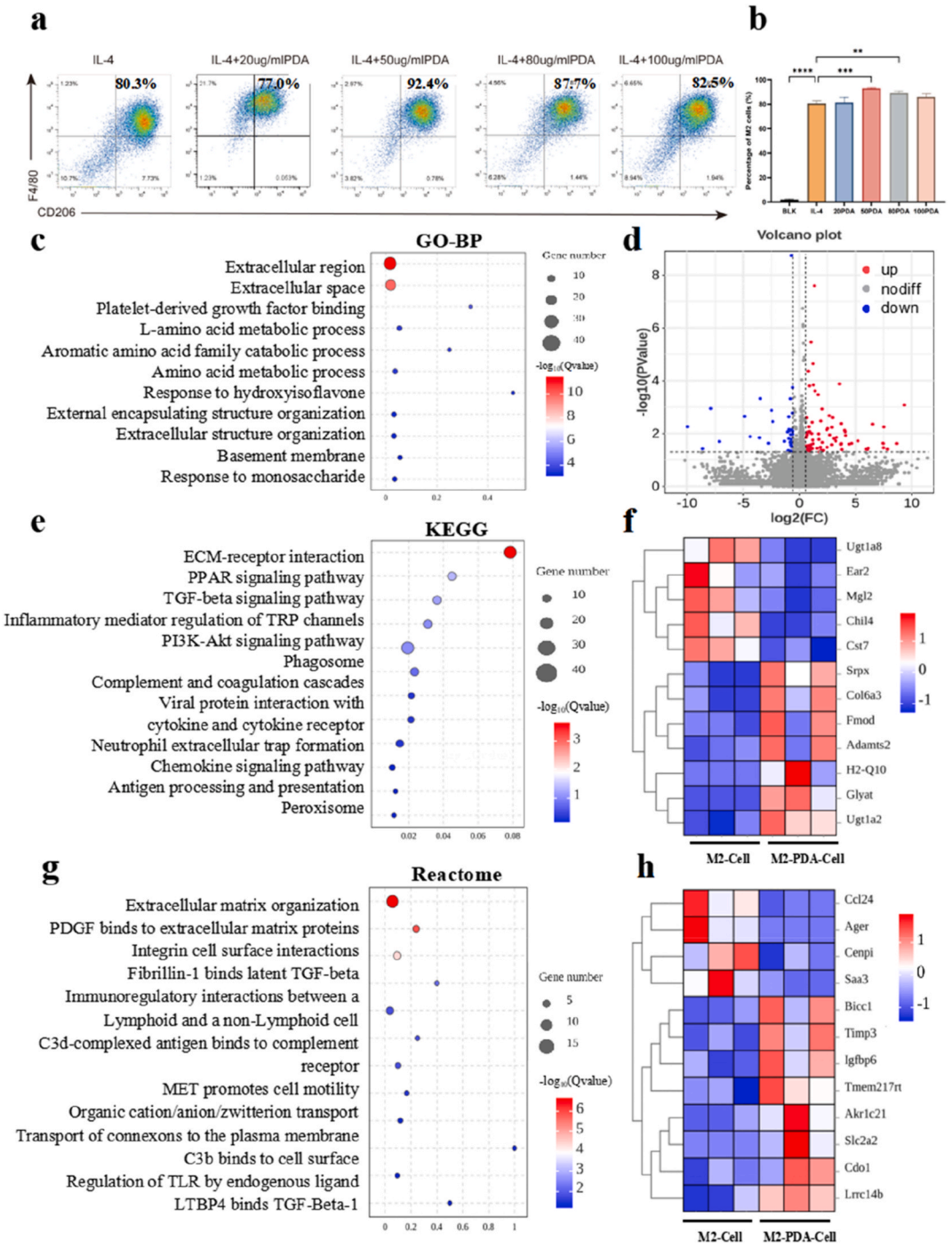

Fig. 4. **(a–b)** Flow cytometry and statistical plots of M2 proportion in BMDMs stimulated by PDA at different concentrations. **(b)** GO-BP analysis of cell transcriptome sequencing with and without PDA stimulation. **(c)** Gene volcano plot of cell transcriptome sequencing with and without PDA stimulation. **(d)** KEGG analysis of cell transcriptome sequencing with and without PDA stimulation. **(e)** Gene expression heatmap of cell transcriptome sequencing related to immune regulation. **(f)** Reactome pathway analysis of cell transcriptome sequencing with and without PDA stimulation. **(g)** Gene expression heatmap of cell transcriptome sequencing related to inflammatory diseases.

protein interaction with cytokine and cytokine receptor and immune modulation (Fig. 4d, Fig. S3b). Notably, in PDA-treated cells, key genes linked to inflammatory diseases (*AGER*, *CCL24*, *SAA3*) fell, while those tied to antioxidant regulation (*AKR1C21*, *CDO1*, *MEP1A*) and immune modulation (*LRRC14B*, *TMEM72*, *Fcrl2*) rose (Fig. 4e and g). Through multi-level gene verification, including transcriptome sequencing and real-time quantitative PCR analysis, the results showed that compared with M2 EXO group, the expression of AGER in M2/pEXO treatment group was significantly decreased, while the expression of AKR1C21 was significantly increased (Fig. S4a and S4b). Further in vivo and in vitro functional experiments confirmed that M2/pEXO treatment has significant therapeutic effect on SLE, which may alleviate the immune disorder and tissue damage of SLE by regulating AGER mediated inflammatory signaling pathway and AKR1C21 related metabolic reprogramming. These findings provide multilayered molecular evidence for M2/pEXO as a new therapeutic strategy for SLE. To evaluate the effect of M2/pEXO on macrophage polarization, the researchers analyzed the mRNA expression levels of M1-and M2-associated markers

using qPCR. Compared with the M2 EXO group, mice treated with M2/pEXO showed significantly increased mRNA levels of the M2-associated markers Arg-1 and Mrc-1, whereas the expression of the M1-associated markers Nos2 and IL-12 was significantly reduced (Fig. S4c–f). These results indicate that M2/pEXO effectively shifts the splenic immune environment toward an M2-dominant, anti-inflammatory phenotype. Overall, PDA stimulation of BMDMs may boost M2 macrophage levels by enhancing intrinsic cellular immune regulation.

2.4. Biocompatibility, antioxidant capacity, and anti-inflammatory function of M2/pEXO

Biocompatibility is of great significance, then cell viability was detected by live/dead staining and CCK8 assay. The data revealed no statistically significant disparity in cell viability between the M2/pEXO-treated and the blank control groups, with cell viability even exceeding 95% at high concentrations (Fig. 5a). Under the fluorescence microscope, the intensity of green fluorescence (live cells) in the treated group showed a pronounced increase compared with red fluorescence (dead cells), indicating a higher cell viability in the treated group (Fig. 5b, Fig. S1d). The natural loading method achieves bionic packaging through the cells' own regulatory mechanisms. While not the most efficient approach, it maximally preserves the biological activity and biocompatibility of exosomes—precisely the characteristics most essential for SLE systemic immunotherapy. The findings demonstrated that M2/pEXO displayed exceptional biocompatibility, remaining non-toxic even at elevated concentrations.

Many studies have revealed that M2 EXO possess the ability to reduce ROS levels, and thereby the ROS scavenging capability of the proposed M2/pEXO was evaluated. As illustrated in Fig. 5d and e, the hydrogen peroxide-treated group exhibited a strong intracellular ROS signal, whereas exposure to exosomes led to a significant reduction in

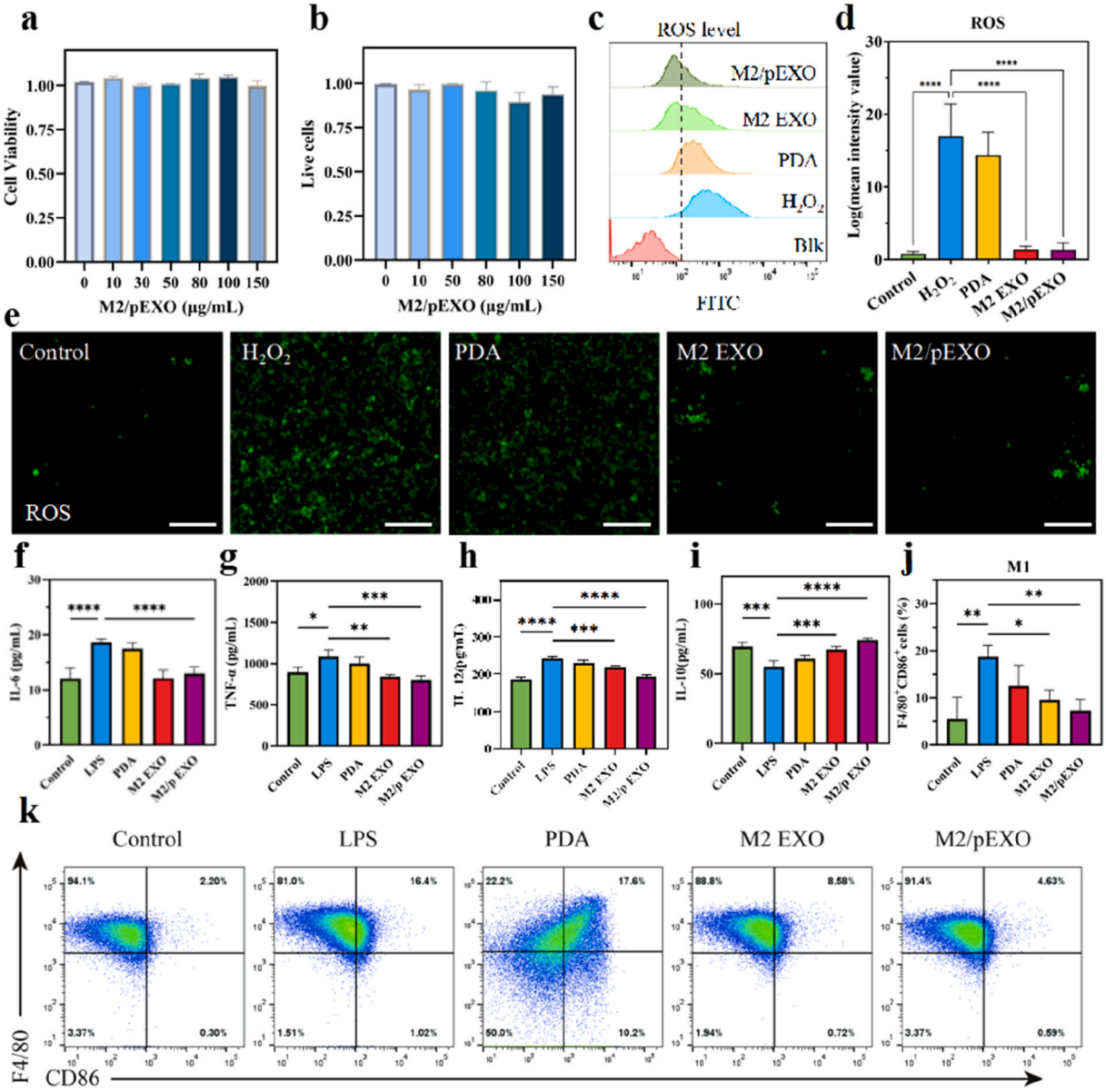

Fig. 5. **(a–b)** Survival of RAW264.7 cell cultures following 12 h treatment with graded doses of M2/pEXO. **(c)** Flow cytometry assessment of ROS levels in RAW264.7 stimulated with different concentrations of M2/pEXO. **(d)** Fluorescence -based statistical analysis of ROS levels in RAW264.7 cells stimulated with different concentrations of M2/pEXO. **(e)** H_2O_2 induced representative intracellular ROS staining of RAW264.7 cells (treated with PDA, M2 EXO and M2/pEXO). Scale bars, 200 μm. **(f–i)** ELISA detection of IL-6, TNF-α, IL-12 and IL-10 levels in different - component cell supernatants under LPS stimulation. **(j–k)** Percentage of $F4/80^+$ $CD86^+$ M1 cells in RAW264.7 Cells by using flow cytometry.

this signal-with M2/pEXO showing the most pronounced effect. Quantitative analysis further confirmed that M2/pEXO could inhibit intracellular ROS intensity by up to one-fold. Moreover, flow cytometric analysis was employed to quantify the ROS-scavenging capacity of M2/pEXO. Consistent with the fluorescence data, M2/pEXO demonstrates the potent antioxidant capability (Fig. 5c, Fig. S5a-c). ROS induce transcriptional activation of inflammatory cytokines. Thus, ELISA assay was performed to measure specific cytokine concentrations. The results showed that both M2 EXO and free PDA inhibited LPS - induced production of TNF -αand IL-6, with M2/pEXO exhibiting the most pronounced inhibitory effects, leading to a 35.37% decrease in TNF-αlevels and a 37.57% decrease in IL-6 levels (Fig. 5f–i, Fig. S7a-b). Further analysis revealed that M2 EXO and free PDA moderately upregulated the anti-inflammatory cytokine IL-10 and downregulated the pro-inflammatory cytokine IL-12, whereas M2/pEXO showed significantly greater effects on both IL-10 upregulation and IL-12 downregulation compared to either M2 EXO or free PDA alone. These findings indicate that the anti-inflammatory effect of M2/pEXO exceeds the simple additive effects of its individual components, demonstrating a synergistic enhancement. Macrophage polarization reflects their inflammatory status, with an increased M1 population signifying elevated inflammation. Therefore, the influence of M2/pEXO on macrophage M1 polarization was examined. Flow cytometry results indicated that, in contrast to the vehicle group, the proportion of M1 macrophages ($F4/80^{+}CD86^{+}$) in the M2/pEXO-treated group was markedly reduced, decreasing from 16.4% to 4.63%. (Fig. 5j and k). This suggests that M2/pEXO can decrease the

proportion of M1 cells and possesses superior antioxidant capabilities.

2.5. Biodistribution and safety of M2/pEXO in an SLE mouse model

To determine whether M2/pEXO exhibits superior antioxidant capacity in the more complex in vivo milieu, biodistribution studies and

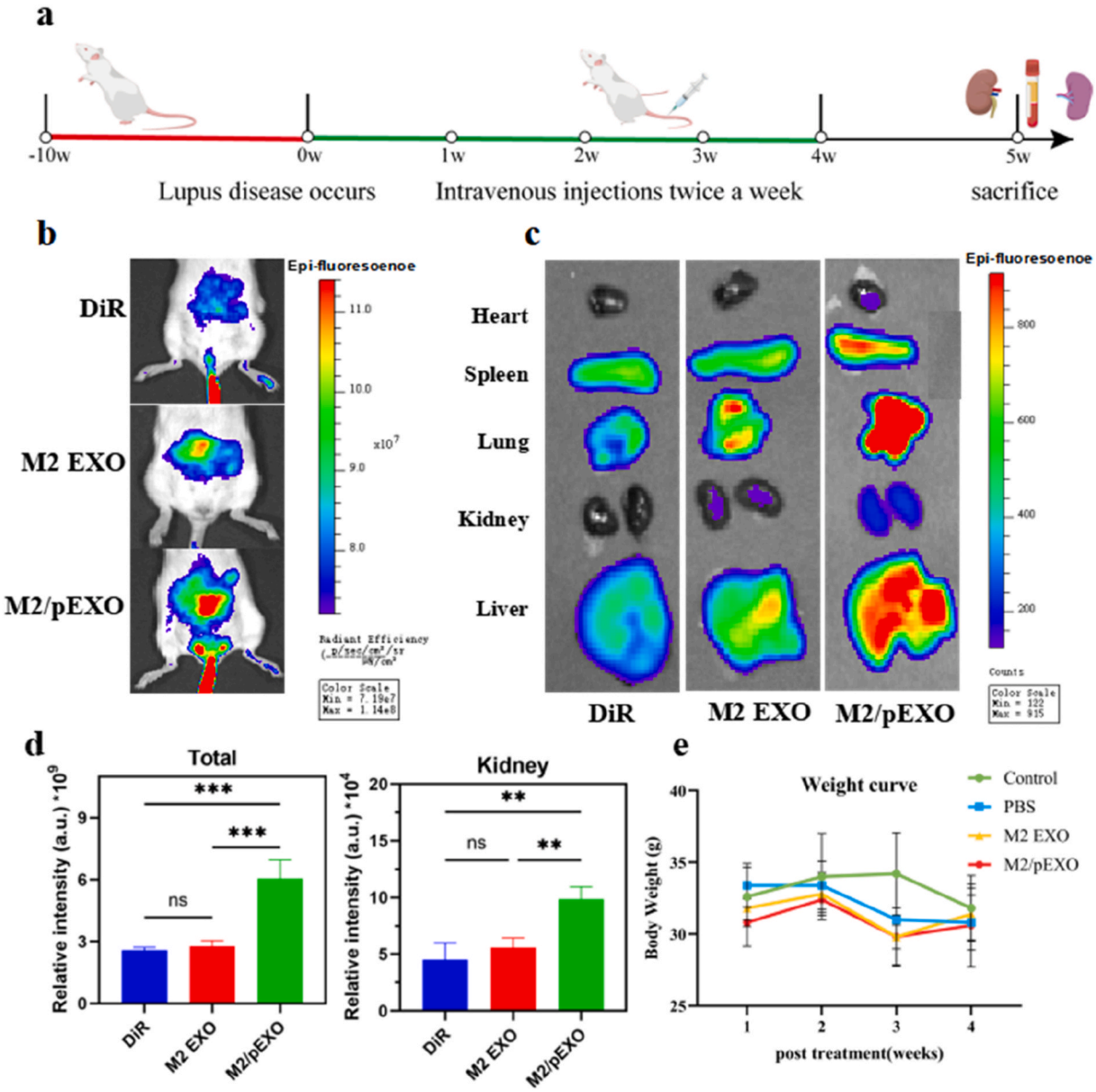

Fig. 6. (a) Illustrative timeline of SLE model induction and therapeutic regimen. **(b–d)** Animals were subjected to i.v. injection of DiR-labeled M2 EXO, M2/pEXO, or free DiR (control). **(b–c)** Ex-vivo imaging of whole-organ panels. **(d)** Semi-quantitative assessment of isolated-organ images. Fluorescence intensities, normalized to overall radiant flux of organ, were extracted via ROI-based analysis in Living Image software. **(e)** Weight curves of mice in different treatment groups.

intravital imaging were performed in mice. M2 EXO and M2/pEXO were labeled with DiR and administered intravenously for optical imaging; free DiR served as the blank control. As shown in Fig. 6b and c, the brightest signals, corresponding to the kidneys and spleen, were detected in the lower abdominal region 24 h post-injection, with the highest DiR signals in mice injected with M2/pEXO. Ex vivo vital imaging of excised tissues demonstrated predominant renal and splenic accumulation of M2/pEXO within 24 h (Fig. 6b). Semi-quantitative ex

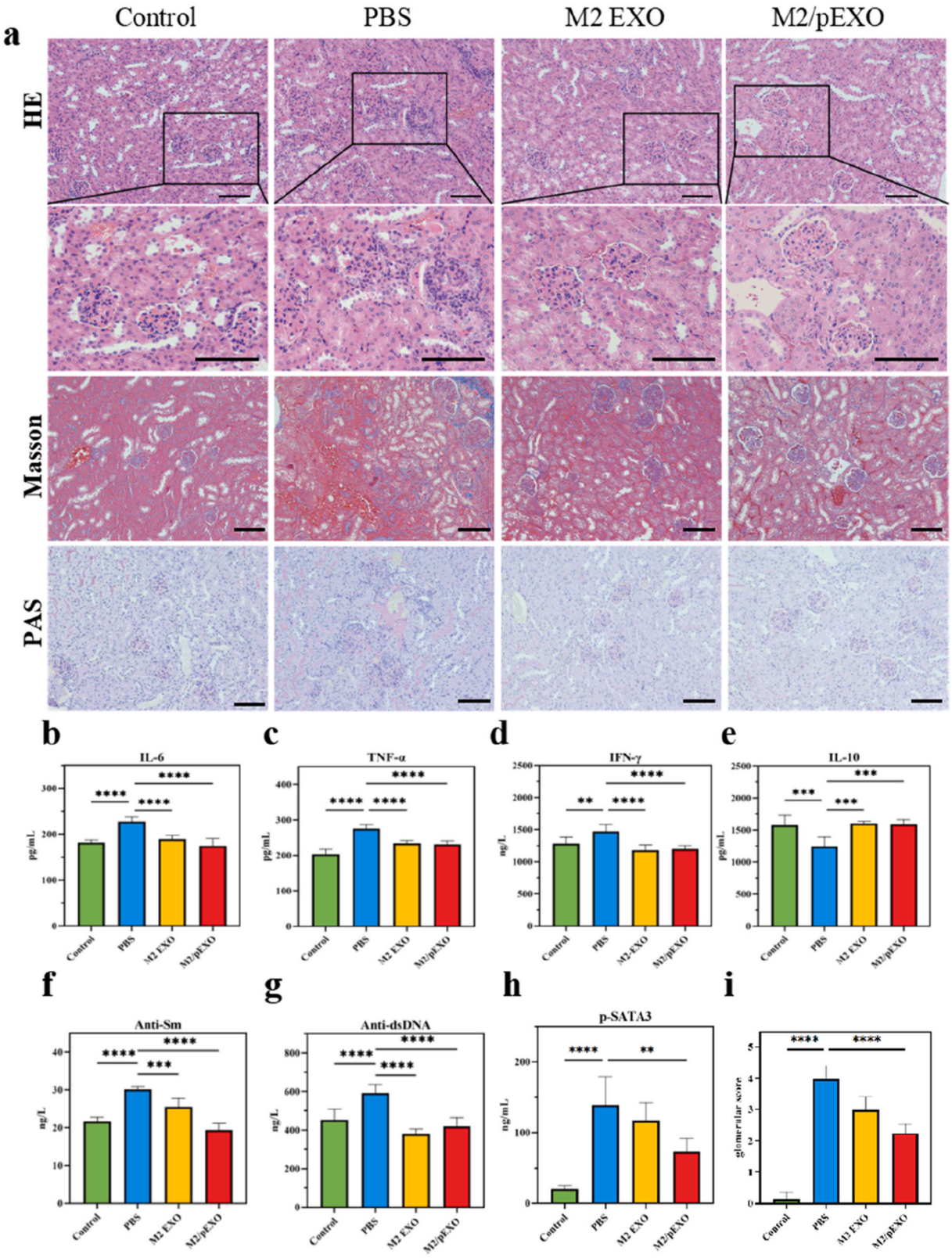

Fig. 7. **(a)** Typical micrographs of renal sections subjected to H&E, Masson and PAS staining. Scale bars, 100 μm. **(b–h)** Elisa was used to detect the levels of IL-6, TNF-α, IFN-γ, IL-10, anti-Sm, anti-dsDNA in plasma and p-STAT3 in tissue lysates. **(i)** Histogram of glomerular scores in different treatment groups.

vivo imaging, adjusted to organ mass, indicated predominant splenic and renal uptake, trailed by pulmonary and hepatic signals (Fig. 6c). Aligning with whole-animal imaging, renal DiR fluorescence in M2/pEXO-treated mice exceeded M2 EXO levels by 2.18-fold (Fig. 6d). In mouse models, the spleen and kidneys serve as primary inflammatory target organs, exhibiting heightened vascular permeability and harbouring substantial accumulations of activated immune cells. Combined in vivo and in vitro studies confirm that M2/pEXO exhibits higher accumulation levels in the kidneys than M2 EXO, indicating longer retention times in vivo and establishing it as a superior antioxidative nanoscavenger. Body-weight change, a key indicator of systemic toxicity, showed no significant inter-group differences over 4 weeks (Fig. 9g), implying the formulation is non-toxic to mice.

2.6. *Therapeutic efficacy and immunomodulatory effects of M2/pEXO in SLE mice*

Subsequently, the curative efficacy of M2/pEXO was assessed in vivo

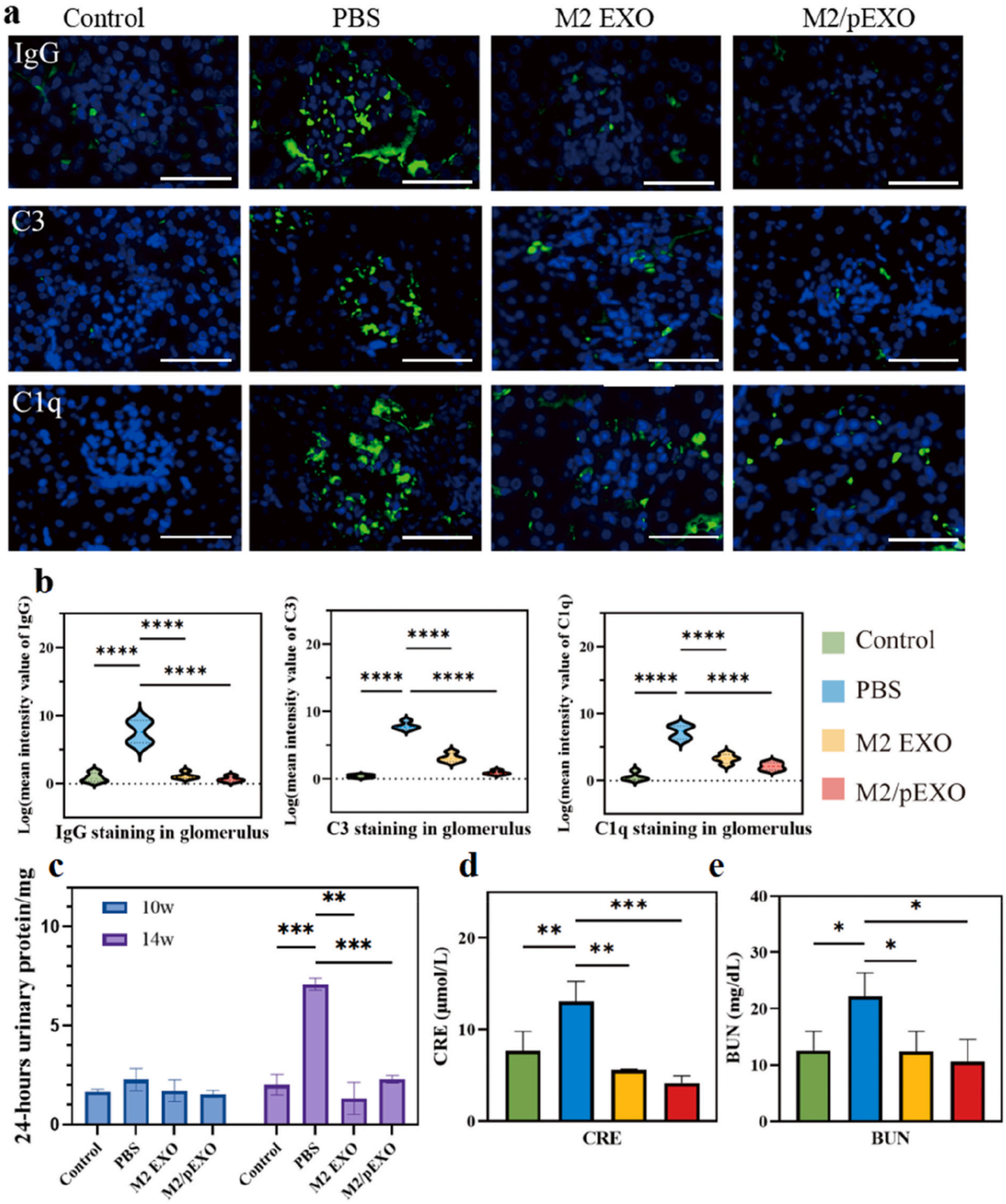

Fig. 8. (a) Typica images demonstrating glomerular immunostaining for IgG, C3, and C1q. Scale bars, 50 μm. **(b)** Immunofluorescence statistics of mouse kidney after different treatments. **(c)** Measurement of total protein in 24-h urine samples was performed via the BCA assay. **(d–e)** Creatinine (d) and blood urea nitrogen (e) levels in mouse plasma with different treatments.

using murine SLE model. PBS (control group), M2 EXO, or M2/pEXO were intravenously injected into 10-week-old MRL/lpr mice every 4 days (Fig. 6a). Lupus nephritis is one of the major complications following inflammatory kidney injury during the progression of SLE [27, 28]. PAS and Masson staining were employed to visualize glomerular basement-membrane glycoprotein deposits and mesangial-matrix collagen proliferation, enabling quantitative assessment of glomerulosclerosis and tissue fibrosis in SLE. Histopathology revealed that saline-treated SLE mice developed severe diffuse proliferative glomerulonephritis characterized by marked mesangial cell proliferation,

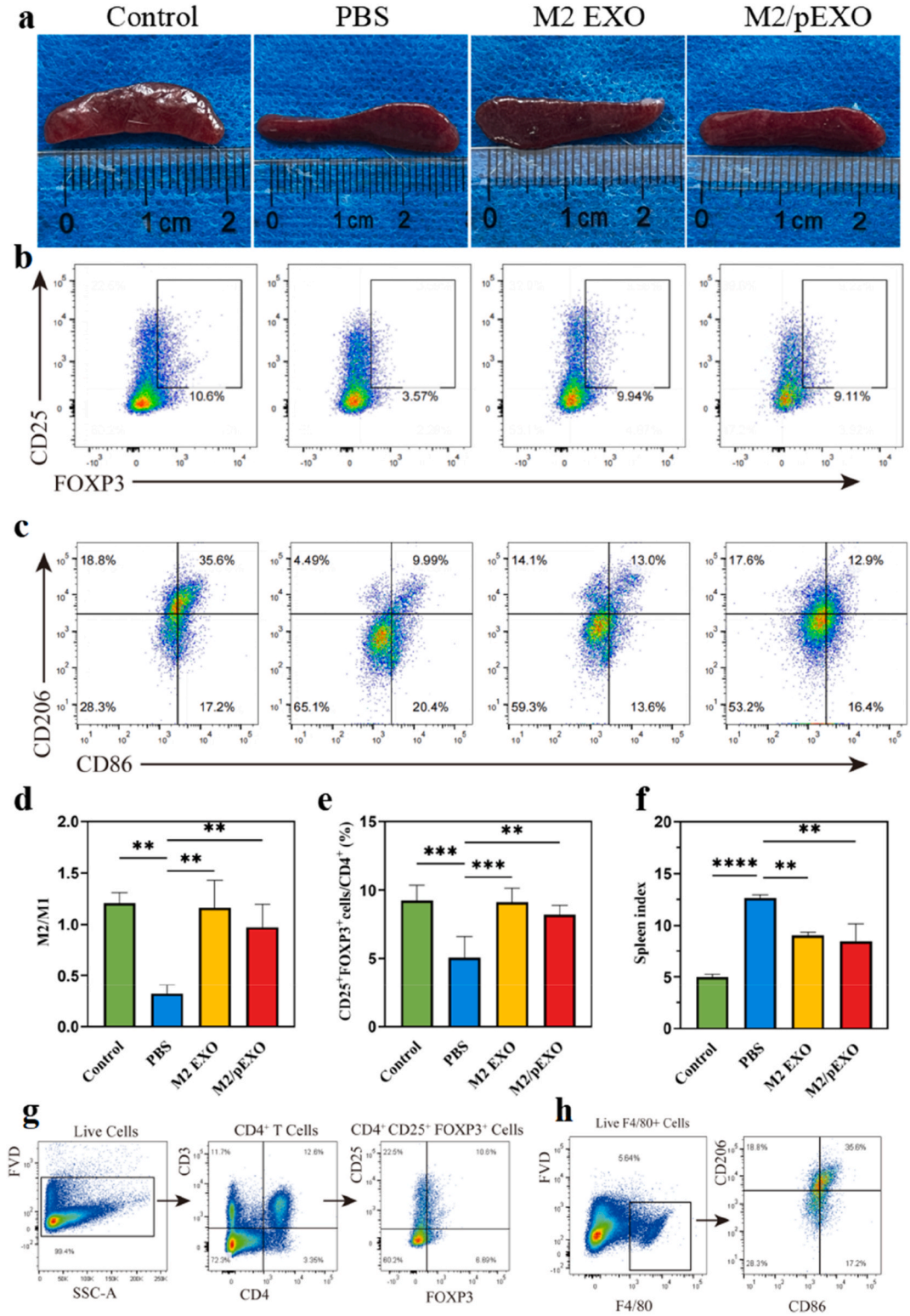

Fig. 9. **(a)** Display of spleen size in mice after different treatments. **(b, e)** The percentage of $CD25^{+}Foxp3^{+}CD4^{+}$ Treg cells in spleen by using flow cytometry. **(c–d)** The proportion of $F4/80^{+}$ $CD86^{+}$ M1 cells and $F4/80^{+}$ $CD206^{+}$ M2 cells in spleen by using flow cytometry. **(f)** Spleen index of mice after different treatments. **(g-h)** Flow cytometry gating strategy for Tregs and macrophages.

neutrophil infiltration, mesangial matrix thickening, diffuse glomerular hyperplasia with focal sclerosis and basement membrane rigidity (Fig. 7a). In contrast, the M2/pEXO group exhibited minimal inflammatory cell accumulation within the kidney interstitium and the least glomerular mesangial enlargement, with virtually no pathological damages observed, thereby attesting to the potent treatment effectiveness of M2/pEXO. The differences in glomerular scores among groups were statistically significant, further confirming the protective effect of M2/pEXO against glomerular pathology in SLE mice (Fig. 7i). Furthermore, serum pro- and anti-inflammatory cytokine levels were assessed in SLE mouse groups given distinct formulations. The highest levels of IL-6, TNF-α and IFN-γ were observed in the saline-treated mice, while M2/pEXO displayed superior inhibitory potency relative to the intermediate response of M2 EXO. (Fig. 7b–d). Besides, the highest anti-inflammatory cytokine IL-10 level was assessed within the M2/pEXO cohort (Fig. 7e). Anti-dsDNA autoantibodies rank among the most disease-specific serological biomarkers in SLE [29], and their elevation indicates increased disease activity. Therefore, serum anti-dsDNA and anti-Sm antibody levels were subsequently carried out. The results showed that elevated serum anti-dsDNA titers indicated severe disease activity in untreated controls, whereas M2/pEXO markedly reduced both anti-dsDNA and anti-Sm antibody levels. (Fig. 7f and g). Sustained over activation of STAT3 is a key transcription factor that mediates inflammation and autoimmune response. In order to further verify the M2/pEXO sequencing related genes, ELISA was used to detect the content of p-STAT3, the activated form of STAT3, in the kidney tissue lysates of mice with different components. The results showed that the expression of p-STAT3 (phosphorylated signal transducer and activator of transcription 3) was significantly decreased in the M2/pEXO treatment group, which had important pathophysiological significance for the treatment of SLE (Fig. 7h).

Complement proteins C1q, C3 and immunoglobulin G (IgG) in kidney tissue directly indicates a high level of inflammatory activity in SLE [30], and thereby their deposition was assessed by immunofluorescence staining. The results showed that accumulation of IgG, C3 and C1q was rarely observed in the M2/pEXO group, with levels even inferior to levels observed in the M2 EXO group (Fig. 8a). The quantitative analysis corresponded to the fluorescence data. The deposition of IgG, C3, and C1q in the M2/pEXO cohort exhibited a pronounced downward shift against the control cohort (Fig. 8b). Urine was collected from the mice, and urinary protein levels were measured to assess kidney function [31]. The results showed significantly diminished proteinuria in the M2/pEXO-treated mice relative to all other groups (Fig. 8c). Simultaneously, glomerular filtration performance was assessed. M2/pEXO as a superior antioxidative nanoscavenger markedly reduced blood urea nitrogen (BUN) and serum creatinine (CRE) concentrations relative to PBS-treated group (Fig. 8d and e).

The lupus-like phenotype of MRL/LPR mice presents with lymphadenopathy, splenomegaly, autoantibody generation, and immune complex-mediated glomerulonephritis. The spleen serves as a critical hub within the immune network, and changes in the spleen index can reflect the activity of the immune network. A decrease of the spleen index indicates a reduction in the level of inflammation to some extent. In comparison with the pathological cohort, the spleen index in M2/pEXO cohort decreased, indicating a reduction in the level of inflammation (Fig. 9f). However, spleen size alone does not quantitatively reflect systemic inflammation. Therefore, Treg, M1, and M2 levels were assessed to monitor the degree of inflammation. Tregs, characterized by high CD25 and transcription factor Foxp3 expression, suppress excessive immune responses. Therefore, surface CD25/Foxp3 on splenic Tregs and F4/80/CD206 on macrophages were examined to evaluate immunomodulatory efficacy. As demonstrated by flow cytometric analysis, M2/pEXO induced a significant upregulation of FOXP3 on splenic Treg cells and CD206 on macrophages, thereby confirming the results of the quantitative analysis (Fig. 9b–e). Therefore, the inhibitory effect of M2/pEXO on macrophages and the promoting effect on Treg cells were verified in vivo.

Biosafety is paramount and a systematic evaluation of the biosafety of M2/pEXO was conducted. First, H&E staining assessed tissue integrity and architecture: microscopy revealed intact hepatic lobules with orderly hepatocytes and no edema or steatosis; normal splenic red/white pulp ratios without fibrosis or necrosis; neatly arranged cardiac muscle fibers; and intact alveolar walls free of exudate (Fig. S6). Collectively, these data confirm that M2/pEXO exerts no overt toxicity to heart, liver, spleen or lung at the administered dose, demonstrating favorable preclinical safety. Additionally, liver and kidney function were evaluated via serum biochemistry: ALT, AST, BUN and CREA all remained within normal reference ranges, M2/pEXO versus control comparisons yielded no statistical significance (Fig. S7c–e), indicating intact hepatic and renal function. Taken together, the antioxidative nanoscavenger delivery system shows excellent biosafety under the experimental conditions.

3. Conclusion

In the present work, we engineered an innovative antioxidative nanoscavenger, an auto-loaded polydopamine-M2 exosome system (M2/pEXO), for systemic lupus erythematosus (SLE) therapy. This platform was constructed through the autonomous uptake of ultrasmall polydopamine (PDA) nanoparticles by BMDMs, followed by exosomal encapsulation during M2 polarization. Notably, PDA itself facilitated the repolarization of M0 macrophages toward an immunoregulatory, M2-like phenotype. The resulting M2/pEXO complex exhibited higher protein content than conventional M2 exosomes, reflecting its naturally engineered, multifunctional composition. Proteomic and functional studies revealed that M2/pEXO enhances antioxidative and anti-inflammatory responses by modulating key pathways related to oxidative stress, mitochondrial oxidative phosphorylation, and immune signaling. Compared with standard M2 EXO, M2/pEXO more effectively suppressed M1 macrophage polarization and the release of inflammatory cytokines such as IL-6, TNF-α and IL-12, while promoting regulatory T cell (Treg) expansion. This integrated activity underscores its utility as a versatile, low-immunogenicity nanoscavenger. In vivo, M2/pEXO significantly alleviated lupus nephritis pathology, as demonstrated by reduced renal immune cell infiltration, attenuated mesangial proliferation, decreased proteinuria, lower serum creatinine, and diminished anti-dsDNA autoantibody levels—all without detectable systemic toxicity. The key advancement offered by the PDA component is the elevation of M2 exosomes from a canonical anti-inflammatory carrier to a synergistic therapeutic system that combines targeted delivery, antioxidative scavenging, and immunomodulation. This multifunctional synergy resulted in comprehensive protective effects against SLE in a complex disease model. We believe that this auto-loaded, naturally assembled composite system represents a promising new avenue for treating SLE and other chronic inflammatory diseases, leveraging the innate bioactivity of M2 exosomes together with the antioxidative and immunomodulatory properties of PDA in a safe, efficient, and clinically translational nanoscavenger platform.

4. Materials and methods

4.1. Materials

Dopamine hydrochloride was supplied by Sigma-Aldrich. Reduced glutathione (GSH) was obtained from Aladdin. Tris-HCl (pH 8.5) was purchased from Beyotime Biotechnology. DTNB (5,5′-dithiobis-(2-nitrobenzoic acid)).

4.2. Preparation of PDA

20 mg Dopamine (DA) was taken up in 10 mL Tris hydrochloride solution at pH 8.5, and kept stirring at 20–25 °C for 2 min. GSH 24 mg

was added and stir at 20–25 °C for 2 h. Subsequently, 31 mg of DTNB was incorporated into the mixture, followed by stirring at 20–25 °C for an additional hour. The resulting solution was dialyzed using a 1 kDa molecular weight cutoff dialysis bag and then freeze-dried for one day to obtain the PDA.

4.3. Cell culture

Bone marrow-derived cells harvested from the long bones of BALB/c mice were induced to differentiate into BMDMs using M-CSF-supplemented complete medium. Following a 7-day culture period, BMDM purity was determined utilizing flow cytometric analysis. Murine RAW264.7 cells were maintained in Dulbecco's Modified Eagle's Medium with high glucose containing 10% FBS (fetal bovine serum, Gibco, USA) and 1% pen/strep (Hyclone). All cells were grown under standard conditions of 37 °C and 5% CO, humidified incubator.

4.4. Collection of M2 exosomes

To isolate M2 EXO, BMDMs were first seeded at a density of 2.0×10^6 cells per well and stimulated with 20 ng/mL interleukin-4 (IL-4, Peprotech, USA) in serum-free medium for 24 h to polarize them into M2 phenotype. M2-polarized BMDMs were cultured to 70-80% confluence, and then maintained in fresh serum-free medium for another 24 h. The cell culture supernatant or biofluid was first subjected to differential centrifugation steps ($300\times g$, $2000\times g$, and $10{,}000\times g$) to remove cells, debris, and apoptotic bodies. The resulting supernatant was then ultracentrifuged (typically at $110{,}000\times g$ for 70 min) to pellet the crude extracellular vesicles. The final pellet was resuspended in a suitable volume of PBS and stored at −80 °C. All centrifugation steps were carried out at 4 °C.

4.5. Preparation of M2/pEXO

PDA solution was first incubated at room temperature for 20 min. Subsequently, dropwise addition of 6.68 μL of the PDA mixture to M2 macrophages was performed. Subsequently, a 24 h co-incubation period at 37 °C was allotted for complex-cell interaction. Afterward, the medium containing unbound PDA mixture was removed, and the cells were maintained in new lacking serum medium for an additional 24 h to induce exosome secretion. Exosomes were then isolated following the protocol described in *Collection of M2 exosomes*.

4.6. Cellular uptake of M2/pEXO

The cellular uptake of M2/pEXO was evaluated using the DiL dye. Exosomes were resuspended in PBS and incubated with DiL dye for 15 min. Labeled exosomes were pelleted by centrifugation at $150{,}000\times g$ to remove unbound dye. RAW264.7 cells were then incubated with DiL-labeled exosomes in the dark for 48 h. After incubation, cells were fixed with 4% paraformaldehyde for 30 min at room temperature, and cell nuclei were labeled with DAPl. Cellular uptake of M2/pEXO was visualized using a Zeiss fluorescence microscope and quantified by flow cytometric analysis.

4.7. Statistical analysis

Data were analyzed using GraphPad Prism 8 software. Results are presented as the mean ± SD. For comparisons between two groups, two-tailed unpaired t tests were used. For multiple group comparisons, one-way analysis of ANOVA was applied. The Mann-Whitney *U* test was used for normally distributed data or data with unequal variances between two groups. A P value < 0.05 was considered statistically significant.

Fundings

This work was supported by the Natural Science Foundation of Nantong Municipality (JC2024029), National Natural Science Foundation of China (82102233), Natural Science Foundation of Jiangsu Province (BK20241838), Jiangsu Funding Program for Excellent Postdoctoral Talent (N/A), Jiangsu Shuangchuang Talent Program (JSSCRC2024596), Jiangsu Provincial Medical Key Discipline Cultivation Unit (JSDW202205), Science and technology Project of Nantong City (XNBH00031655), Science and technology Project of Nantong City (JC2023037). We are grateful to Professor Yuanjin Zhao from Southeast University, China for his guidance and support.

CRediT authorship contribution statement

Huiyuan Ye: Data curation, Formal analysis, Methodology, Software, Visualization, Writing – original draft, Writing – review & editing. **Shufan Hou:** Methodology, Software, Validation. **Xingyu Li:** Resources, Software. **Yujuan Zhu:** Conceptualization, Funding acquisition, Project administration, Resources, Supervision. **Zhifeng Gu:** Funding acquisition, Project administration, Resources, Supervision, Validation. **Mei Yang:** Funding acquisition, Software.

Declaration of competing interest

The authors declare that they have no known competing financial interests or personal relationships that could have appeared to influence the work reported in this paper.

Appendix A. Supplementary data

Supplementary data to this article can be found online at https://doi.org/10.1016/j.mtbio.2026.103199.

Data availability

Data will be made available on request.

References

[1] C. Mohan, et al., Nat. Rev. Nephrol. 19 (8) (2023) 491.
[2] E. Patiño-Martinez, M.J. Kaplan, Nat. Rev. Rheumatol. 21 (7) (2025) 377.
[3] M. Scherlinger, et al., Nat. Rev. Drug Discov. 24 (2025) 926.
[4] S.J. Allison, Nat. Rev. Nephrol. 18 (9) (2022) 543.
[5] S. Caielli, et al., Annu. Rev. Immunol. 41 (2023) 533.
[6] G.C. Tsokos, Nature 611 (7936) (2022) 456.
[7] M.R.W. Barber, et al., Nat. Rev. Rheumatol. 17 (6) (2021) 307.
[8] C.A. Wagner, J.A. James, Nat. Rev. Rheumatol. 21 (8) (2025) 439.
[9] C. Law, et al., Nature 631 (8022) (2024) 857.
[10] R. Isaac, et al., Cell Metab. 33 (9) (2021) 1744.
[11] J.J. Lai, et al., Adv. Sci. (Weinh.) 9 (15) (2022) e2103222.
[12] R. Kalluri, V.S. LeBleu, Science (6478) (2020) 367.
[13] J. Rezaie, et al., Cell Commun. Signal. 20 (1) (2022) 145.
[14] C. Villa, et al., Nat. Nanotechnol. 19 (10) (2024) 1532.
[15] S. Shin, et al., Nat. Mater. 22 (5) (2023) 656.
[16] T.K. Kishimoto, et al., Nat. Nanotechnol. 11 (10) (2016) 890.
[17] A. Cifuentes-Rius, et al., Nat. Nanotechnol. 16 (1) (2021) 37.
[18] Z. Zhen, et al., Mater. Today Bio 34 (2025) 102156.
[19] N. Feliu, W.J. Parak, Science 384 (6694) (2024) 385.
[20] B.R. Smith, S.S. Gambhir, Chem. Rev. 117 (3) (2017) 901.
[21] N. Joudeh, D. Linke, J. Nanobiotechnol. 20 (1) (2022) 262.
[22] C. Liu, et al., Chem. Soc. Rev. 54 (2025) 8434.
[23] S. Ma, et al., Adv. Sci. (Weinh.) 10 (16) (2023) e2207768.
[24] Y. Xu, et al., ACS Nano 16 (4) (2022) 5932.
[25] G. Gupta, et al., ACS Nano 17 (17) (2023) 17451.
[26] M. Dehshiri, et al., Nanomedicine 68 (2025) 102837.
[27] D. McCluskey, et al., Cell Rep. Med. 6 (8) (2025) 102247.
[28] H. Wang, et al., Nat. Commun. 16 (1) (2025) 4686.
[29] J.J. Wang, et al., Autoimmunity 58 (1) (2025) 2441992.
[30] S.C. Choi, et al., Sci. Transl. Med. 12 (2020) 551.
[31] V. Navarro-Sánchez, et al., Nephrol. Dial. Transplant. 41 (3) (2025) 511.